N95- 22440

Fundamental mechanisms in premixed flame propagation via vortex-flame interactions - numerical simulations

By T. Mantel

1. Motivation and objectives

During the past few years, direct numerical simulations (DNS) have been extensively used to study turbulent reacting flows in order to obtain a better understanding of the interaction between a turbulent flow field and a flame front, mainly for modeling purposes. We can cite different studies with increasing degree of complexity. Three-dimensional DNS of a decaying isotropic turbulence with chemical reactions (no heat release and constant density) have been carried out by Picart *et al.* (1988), Rutland *et al.* (1990), El Tahry *et al.* (1991). More recently, heat release and variable density have been taken into account by Poinsot *et al.* (1991), who have analyzed the interaction between a two-dimensional vortex pair and a premixed laminar flame. Haworth & Poinsot (1992) and Trouvé & Poinsot (1994) focused their attention on the effects of the Lewis number by studying the interaction between (respectively) a two- and three-dimensional decaying homogeneous turbulence and a premixed flame front. We can also note the work of Poinsot *et al.* (1994), who performed a two-dimensional interaction between a turbulent flame front and a cold wall.

Due to the limitations of the available computers, all the studies cited above have been performed using a one-step irreversible reaction (Reactants → Products) to describe the chemistry occurring in a flame. Consequently, some conclusions of these studies remain questionable due to complex chemistry effects. This last remark is supported by the work of Baum *et al.* (1992), who have studied the interaction between a two-dimensional decaying isotropic turbulence and a stoichiometric hydrogen-air premixed flame using the 9 species, 19 reactions scheme of Miller *et al.* (1982). Despite the Lewis number (based on H_2) of their simulation being definitely less than unity, the local flamelet speed S_n decreases with increasing tangential strain rate, which corresponds to the behavior of a flame having a Lewis number greater than unity (Clavin 1985, Law 1988). The Lewis number is defined as the ratio of the thermal diffusivity (in the fresh gases) α_u and of the molecular diffusivity of the limiting species $\mathcal{D}$: $Le = \alpha_u/\mathcal{D}$. Moreover, they find a better correlation between the tangential strain rate and S_n rather than the local curvature and S_n.

This contradicts partially the previous work of Haworth & Poinsot (1992), who studied the same configuration using a one-step Arrhenius chemistry. In that study, they observe that the curvature seems to be the determinant parameter controlling the local flame structure. They notice a strong correlation between the curvature and the local flame velocity S_n for all the Lewis numbers investigated ($Le = 0.8$,

1.0, and 1.2). For the tangential strain rate, they found a significant correlation (with S_n) for $Le = 1.0$.

This short discussion points out the need to verify the limit of validity of simple mechanisms able to be implemented in DNS codes. Because reduced chemical mechanisms are available and represent a good compromise between (too) simple mechanisms and (unreachable) full chemical schemes, it is of primary interest to investigate the behaviors of some of these models on a configuration which exhibits the fundamental mechanisms occurring in premixed turbulent flames and for which experimental results are available.

The interaction between vortex pairs or ring vortices and a premixed planar flame possesses the major features encountered in turbulent premixed combustion such as unsteadiness, stretch, curvature, Lewis number, radiative heat losses, and complex chemistry effects. This simplistic configuration has been previously studied both experimentally and numerically for different purposes by several authors (Poinsot *et al.* 1991, Rutland & Ferziger 1991, Lee *et al.* 1993, Roberts *et al.* 1992-1993, Samaniego *et al.* 1994-b, Driscoll *et al.* 1994). Some of these works have focused their attention on the effects of radiative heat losses and of the strain on the quenching of a premixed flame. The motivation of these studies was to propose an update of the premixed turbulent combustion diagrams to clarify the limit between the flamelet and non-flamelet combustion regimes (Poinsot *et al.* 1991, Roberts *et al.* 1993). Other studies have extracted different statistics of curvature and orientation factors of turbulent premixed flame fronts (Lee *et al.* 1993).

The goal of the present study is to assess numerically the ability of single-step and two-step chemical models to describe the main features encountered during the interaction between a two-dimensional vortex pair and a premixed laminar flame.

This paper represents the second part of a joint experimental and numerical project concerning vortex flame interactions performed at the Center for Turbulence Research. This first part investigated by Samaniégo *et al.* (1994-b) concerns the experimental aspect of this project. Thus, the configuration retained in our study corresponds to the experimental one of Samaniego *et al.* (1994-b). Briefly, it concerns the interaction between a two-dimensional vortex pair generated by acoustic excitation and a V-shaped flame stabilized on a heated wire. In the experiment, imaging of the light emitted by the flame and smoke visualization of the flow field have been carried out to provide initial conditions to the simulation and eventually data to perform quantitative comparisons between the experiment and the simulation. Light emission imaging allows determination of the time history of the flame surface area, of the global heat release, and of the distribution of the heat release along the flame front. The characteristics of the vortex pair (circulation, position of the vortices with respect to the flame, distance between the center of the vortices) are obtained from smoke visualization.

In the two-step mechanism, the reaction kinetics are represented by a first chain branching reaction $A + X \rightarrow 2X$ and a second chain termination reaction $X + X \rightarrow P$ (Zel'dovich 1948). This mechanism has been successfully used to analyze different features of premixed laminar flames (Liñán 1971, Hocks *et al.* 1981, Seshadry and

Peters 1983). In particular, Seshadry and Peters (1983) investigated the response of a premixed laminar flame to an external strain. They pointed out the relative role of the Lewis number for the reactant A and the intermediate species X. In the case of a positive stretch, they show that the high diffusivity of the intermediate species contributes to a decrease of the reaction rate independently of the Lewis number of the reactant species.

This paper presents the fundamental mechanisms occurring during vortex-flame interactions and the relative impact of the major parameters encountered in turbulent premixed flames and suspected of playing a role in quenching mechanism:

- Influence of stretch is investigated by analyzing the contribution of curvature and tangential strain on the local structure of the flame. The effect of Lewis number on the flame response to a strained field is analyzed.

- Radiative heat losses which are suspected to be partially or totally responsible for quenching (Poinsot *et al.* 1991, Roberts *et al.* 1993) are also investigated.

- The effect of the diffusion of radicals is studied using a two-step mechanism in which an intermediate species is present. The parameters of the two-step mechanism are entirely determined from physical arguments.

- Precise quantitative comparisons between the DNS and the experimental results of Samaniégo *et al.* (1994-b) are performed. These comparisons concern the evolution of the minimum heat release rate found along the flame front during the interaction and the distribution of the heat release rate along the flame front.

2. Accomplishments

2.1 The mathematical model

2.1.1 The conservation equations

The DNS code has been developed at the Center for Turbulence Research following the methodology of Lele (1992) and Poinsot & Lele (1992). The code fully resolves the compressible Navier-Stokes equations using a sixth order spatial scheme (Lele 1992) and a third order temporal scheme (Wray 1990). Due to the heat release and the resulting gas expansion, the boundary conditions of the computational domain are inflow/outflow (Poinsot & Lele 1992). The transport equations solved in the DNS code can be written

$$\frac{\partial \rho}{\partial t} + \frac{\partial}{\partial x_j}(\rho u_j) = 0 \tag{2.1}$$

$$\frac{\partial \rho u_i}{\partial t} + \frac{\partial}{\partial x_j}(\rho u_i u_j) = -\frac{\partial p}{\partial x_i} + \frac{\partial \tau_{ij}}{\partial x_j} \tag{2.2}$$

$$\frac{\partial \rho E}{\partial t} + \frac{\partial}{\partial x_j}[(\rho E + p)u_j] = \frac{\partial}{\partial x_j}(u_i \tau_{ij}) + \frac{\partial}{\partial x_j}\left(\lambda \frac{\partial T}{\partial x_j}\right) + \dot{Q} - h(T - T_u) \tag{2.3}$$

where

$$\tau_{ij} = \mu\left(\frac{\partial u_i}{\partial x_j} + \frac{\partial u_j}{\partial x_i}\right) - \frac{2}{3}\mu\frac{\partial u_k}{\partial x_k}\delta_{ij} \tag{2.4}$$

$$\rho E = \frac{1}{2}\rho u_i^2 + \frac{p}{\gamma - 1} \tag{2.5}$$

The transport equation for the species α is classically written:

$$\frac{\partial \rho Y_\alpha}{\partial t} + \frac{\partial}{\partial x_j}(\rho u_j Y_\alpha) = -\frac{\partial \mathcal{J}_j^\alpha}{\partial x_j} + \dot{w}_\alpha \tag{2.6}$$

where $\mathcal{J}_j^\alpha$ is the diffusion of the species α flux modeled using a Fickian approximation and $\dot{w}_\alpha$ the sink term due to chemical reaction.

Here ρE represents the total energy, $\dot{Q}$ is the heat released by chemical reaction per unit mass of fresh gas, the subscript u corresponds to the unburnt gases. ($\dot{Q}$ and $\dot{w}_\alpha$ will be defined in detail later in this section for the one-step and two-step chemical models.) In the energy equation, the heat losses are represented by a term linear in temperature and a heat loss parameter h which will be described later.

The transport properties of the fluid are temperature dependent following a power law:

$$\frac{\mu}{\mu_u} = \left(\frac{T}{T_u}\right)^b \tag{2.7}$$

where μ represents the dynamic viscosity and b is a constant (here $b = 0.76$). The thermal conductivity λ and the molecular diffusivities $\mathcal{D}_\alpha$ for the species are determined by assuming constant Prandtl and Schmidt numbers.

2.1.2 The one-step chemical model

In this model, the chemistry is described by a single step irreversible reaction:

$$\text{A(reactants)} \rightarrow \text{P(products)} \tag{2.8}$$
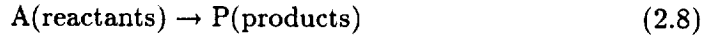
The reaction rate of this reaction is expressed using a classical Arrhenius law. Following the notations of Williams (1985) the reaction rate for the deficient species (subscript A) can be written

$$\dot{w}_A = \Lambda \rho Y_A \exp\left(-\frac{\beta(1 - \Theta)}{1 - \alpha(1 - \Theta)}\right) \tag{2.9}$$

where

$\Theta = (T - T_u)/(T_b - T_u)$ is the reduced temperature;
$\alpha = (T_b - T_u)/T_b$ represents the heat release parameter;
$\beta = \alpha E_a/R^0 T_b$ is the Zel'dovich number;
$\Lambda = B\exp(-\beta/\alpha)$ is the pre-exponential factor.

T_b and E_a represent respectively the temperature in the burnt gases and the activation energy of the reaction, R^0 being the universal gas constant.

The source term $\dot{Q}$ appearing in Eq. 2.3 is

$$\dot{Q} = (-\Delta_f^0)\dot{w}_A \qquad (2.10)$$

where $(-\Delta_f^0)$ is the heat of reaction per unit mass of reactant.

2.1.3 The two-step chemical model

The two-step mechanism initially proposed by Zel'dovich (1948) consists of a first order chain branching reaction and a second-order termination reaction:

$$A + X \rightarrow 2X \qquad (2.11)$$

$$X + X \rightarrow P \qquad (2.12)$$

In the first reaction, two radicals X are created while one radical is consumed during the transformation of the reactant A into X. This initiation step is essential because it provides radicals to initiate chain reactions. This type of reaction is considered as thermo-neutral and has a high activation energy. Then, two radicals recombine to form the product P during the termination step (or chain breaking). This recombination step is highly exothermic and all the energy is release during this step. These approximations are consistent with the simplistic description that the more exothermic a reaction is, the smaller the activation energy.

Thus, using this description and considering equal molecular weight $(W = W_A = W_X)$, the reaction rates for the two reactions are

$$RR_1 = \frac{\Lambda_1}{W}\rho^2 Y_A Y_X \exp\left(-\frac{\beta_1(1-\Theta)}{1-\alpha(1-\Theta)}\right) \qquad (2.13)$$

$$RR_2 = \frac{\Lambda_2}{W}\rho^2 Y_X^2 \qquad (2.14)$$

and for the two species,

$$\dot{w}_A = -\Lambda_1\rho^2 Y_A Y_X \exp\left(-\frac{\beta_1(1-\Theta)}{1-\alpha(1-\Theta)}\right) \qquad (2.15)$$

$$\dot{w}_X = \Lambda_1\rho^2 Y_A Y_X \exp\left(-\frac{\beta_1(1-\Theta)}{1-\alpha(1-\Theta)}\right) - 2\Lambda_2\rho^2 Y_X^2 \qquad (2.16)$$

where

$$\Lambda_1 = \frac{B_1}{W}\exp\left(-\frac{\beta_1}{\alpha}\right) \quad ; \quad \Lambda_2 = \frac{B_2}{W}$$

In the energy equation, the source term due to chemical reactions is

$$\dot{Q} = \sum_{k=1}^{R}(-\Delta H_k^0)RR_k \qquad (2.17)$$

where ΔH_k^0 is the heat released by the kth reaction. In the present case, we consider that the first reaction is thermo-neutral and all the heat is liberated during the second reaction. Thus $\dot{Q}$ becomes

$$\dot{Q} = (-\Delta H_2^0)\frac{\Lambda_2}{W}\rho^2 Y_X^2 \ . \tag{2.18}$$

This mechanism has been utilized in various studies concerning premixed laminar flames. Liñán (1971) proposed to represent a premixed laminar flame as a succession of layers in which different transformations occur. On the unburnt gas side, a thick preheat zone (relative to the laminar flame itself) is present. In this layer, only diffusion and convection phenomena take place and chemical reactions do not exist. Then, the chemistry of the hydrocarbons takes place in a thin layer in which radicals are produced. These radicals are transported (by diffusion and convection towards the burnt gases and by diffusion towards the fresh gases) and recombine into products in a broader layer including the hydrocarbon consumption layer. Different regimes were encountered by Liñán depending on the ratio of the frequency factors of the two reactions Λ_2/Λ_1.

Hocks et al. (1981) investigated the quenching processes related to the interaction between a premixed laminar flame and a cold wall. The authors conclude that the two-step mechanism is able to describe the mechanism leading to flame quenching. It appears that the behavior of the flame close to the wall is strongly dependent on the maximum concentration of the intermediate species, which is essentially determined by the ratio Λ_2/Λ_1.

Later, Seshadry & Peters (1983) studied the structure of a planar premixed laminar flame submitted to stretch. Considering a high activation energy for the first reaction, the authors derived an asymptotic expansion for the temperature. They found that the first order temperature can be expressed as a function of the stretch and the Lewis numbers for the reactant and the intermediate species:

$$T_0^1 = -K^*\left\{\frac{Le_A - 1}{Le_A} + (-\Delta H_2^*)\left[\frac{1 - Le_X}{Le_X}I_0\right]\right\} \ . \tag{2.19}$$

The subscript 0 refers to the axial coordinate where Y_X is maximum, I is a function always positive, K^* is a non-dimensionalized stretch and $(-\Delta H_2^*)$ is the non-dimensionalized heat of reaction of the recombination step. The relation (2.19) points out the respective roles of the diffusivities of the reactant and of the intermediate species. Considering only the first term on the RHS of Eq. 2.19, for positive stretch the temperature decreases (increases) for $Le_A > 1$ ($Le_A < 1$). For $Le_A = 1$, the temperature remains constant equal to the zero order temperature, regardless of the value of the stretch. This recovers the classical conclusions of the role played by the Lewis number of the reactant on stretched flames (Clavin 1985, Law 1988).

The second term on the RHS of (2.19) enhances the effects of diffusivity of the intermediate species on the dynamics of stretched flames. Since radicals are mostly very light species, they have high diffusivities leading to Lewis numbers significantly less than unity. Thus, in case of positive (negative) stretch, the diffusivity of the

intermediate species tends to decrease (increase) the temperature and then the local laminar flame speed. This result points out that even for $Le_A = 1$, the flame can be sensitive to the effect of stretch and exhibits locally a variation of the laminar flame speed.

This brief description shows the ability of the two-step mechanism to describe fundamental phenomena occurring in premixed flames in different configurations. However, it also points out the appearance of new parameters such as the ratio of the frequency factors Λ_2/Λ_1, the Lewis number for the intermediate species, the activation energy and the heat released by each of the two-step mechanism. This represents an infinity of combinations between these parameters. The challenge, then, is to provide this model with a realistic set of parameters representative of the fundamental mechanisms encountered in the kinetics of hydrocarbons.

To do so, we will focus our attention on the hydrogen-oxygen submechanism which is hierarchically the first submechanism (followed by the oxidation of carbon monoxyde) occurring in the chemistry of hydrocarbons (Glassman 1987, Westbrook and Dryer 1984). In this submechanism, the H atoms play a determining role because they provide a major source of radicals in the branching reactions of the oxidation of H_2. Furthermore, the concentration of H radical directly affects the overall heat release and, consequently, the reaction rate (Westbrook and Dryer 1984). In the $H_2 - O_2$ submechanism, one of the most important chain branchings is

$$H + O_2 \rightarrow OH + O .\tag{2.20}$$

In the chain branching reaction (2.20), one H atom is consumed whereas radicals O and hydroxyl OH are produced and contribute to further branching reactions in which H radicals are created such as

$$O + H_2 \rightarrow OH + H$$
$$OH + H_2 \rightarrow H_2O + H$$
$$OH + OH \rightarrow H_2O + O$$
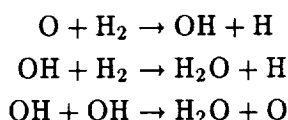
The reaction 2.20 is endothermic of 17 kcal/mol and has an activation energy of 14.4 kcal/mol (Yu *et al.* 1994).

Then, radicals are transformed to form product and liberate energy in chain breaking reaction. In the high temperature regime, a principal termination reaction is

$$H + OH + M \rightarrow H_2O + M ,\tag{2.21}$$
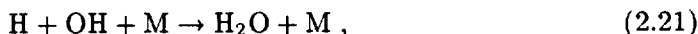
where M is a third body. During this step, radicals H and OH recombine to form products of combustion (here water). This reaction is highly exothermic (120 kcal/mol) and has a zero activation energy.

The rate coefficients for these two reactions are reported in Table 1.

From these considerations, all the parameters appearing in the two-step mechanism 2.11 and 2.12 can be estimated from the rate coefficients reported in Table 1. The ratio of the frequency factors Λ_2/Λ_1 of reactions 2.11 and 2.12 can be determined from the values of B_1 and B_2 and from the temperature of the burnt gases.

| reaction | $k = BT^n e^{-E_A/R^0 T}$ | | | |
	B $(cm^3 mol^{-1} s^{-1})$	n	E_A (kJ/mol)	ref
$HO_2 \rightarrow OH + O$	$8.3 \ 10^{13}$	0	60.3	Yu et al. 1994
$H + OH + M \rightarrow H_2O + M$	$1.6 \ 10^{22}$	-2	0	Miller and Bowman 1984

Table 1. Reacting mechanism, rate coefficients

As we mentioned previously, the H atoms play a determinant role in the chemistry of hydrocarbons. Thus, we will identify the intermediate species X of the two-step mechanism to the H atom which leads to a Lewis number for X, $Le_X = 0.15$. The activation energies of the two-step mechanism are those of the reactions 2.10 and 2.11 reported in Table 1.

2.1.4 Initialization of the two-step mechanism

To initialize the one-dimensional laminar flame using the two-step mechanism, the assumption of quasisteady state for the intermediate species is considered. Thus from Eq. 2.16, the concentration of the radical is directly related to the concentration of the species A and to the temperature:

$$Y_X = \frac{1}{2}\frac{\Lambda_1}{\Lambda_2} Y_A \exp\left(-\frac{\beta_1(1-\Theta)}{1-\alpha(1-\Theta)}\right) \qquad (2.22)$$

We note that using Eq. 2.22 in Eq. 2.15 makes the two-step mechanism (under the assumption of quasi steady state for the intermediate species) reduce to the one-step second-order mechanism,

$$A + A \rightarrow P . \qquad (2.23)$$

2.1.5 The radiative heat loss model

The radiative heat losses are taken into account in the energy equation by a linear term in temperature. The heat loss parameter h appearing in Eq. 2.3 comes from the asymptotic analysis of Williams (1985-pp 271-276). He considers the asymptotic structure of a one-dimensional premixed laminar flame submitted to radiation or conduction to a wall. Considering constant properties for the fluid, Williams proposes

$$h = \frac{l}{2\beta} Pr^2 \lambda \left(\frac{S_L^{ad}}{\nu_u}\right)^2 , \qquad (2.24)$$

where l is a constant and Pr a Prandtl number, ν_u represents the molecular viscosity in the fresh gases and S_L^{ad} the adiabatic laminar flame speed.

2.1.6 Configuration

The configuration retained in this study concerns the interaction between a two-dimensional vortex pair and a planar premixed laminar flame. This geometry corresponds to the experimental device of Samaniego *et al.* (1994). In the experiment, a mixture of methane or propane and air is introduced in a vertical channel of square cross section. The flame is stabilized on a heated wire and exhibits a two-dimensional V-shape. On the left side of the duct, a vortex pair is generated by acoustic excitation and interacts with the flame (see Fig. 1). Then, during the main duration of the interaction, the flow keeps its two-dimensionality. The DNS of all the experimental domain cannot be considered because of the high computational time and memory requirement. Nevertheless, the second flame (on the right of Fig. 1) does not play any significant role during the early stages of the interaction and allows us to consider only the left side of the domain where the interaction occurs (Samaniégo *et al.* 1994). Moreover, one can demonstrate that due to the Gallilean invariance of the Navier-Stokes equations, the problem is equivalent to considering a sub-domain related to the frame of reference of the flame and convected by the mean flow field.

The characteristics of the vortices (circulation, size, distance with respect to the flame, angle of impingement) are obtained from the experiment and are reported in Table 2. Here, the Damköhler is defined by $Da = sS_L^{0^2}/V_D\alpha_u$ and the laminar flame thickness by $\delta_f = \alpha_u/S_L^0$. Three vortex pairs having different circulations and sizes are studied. For each interaction, a methane-air flame and a propane-air flame are investigated in order to study the effects of the Lewis number. The methane-air flame with an equivalence ratio of 0.55 exhibits a Lewis number equal to unity whereas the propane-air flame with an equivalence ratio of 0.50 has a Lewis number of 1.8. The parameters of the different cases analyzed in this study are reported in Table 2.

Since the structure of the vortex has not been precisely determined in the experiment, it is difficult to locate our study in the diagram of flame-vortex interactions proposed by Poinsot *et al.* (1991). Nevertheless, from the PIV measurements of Driscoll *et al.* (1994), the maximum tangential velocity of the vortices u_θ^{max} and the radius of the vortex core σ can be estimated. Driscoll *et al.* determined that $2 \leq u_\theta^{max}/V_D \leq 6$ and $1/2 \leq \sigma/s \leq 1/6$, where V_D is the displacement velocity of the vortex pair and s the distance separating the center of the vortices. Thus, we can roughly locate our study in the quenching region of the diagram represented in Fig. 2.

The temperature jump across the flame front is set exactly equal to 5, leading to the heat release parameter $\alpha = 0.8$.

Vortex pairs can be easily generated numerically, and several authors have proposed analytical solutions that satisfy the Navier-Stokes equations. Among these solutions, one of the most used in numerical simulations are the Oseen vortex (Oseen 1911) and the vortex "hat" used by Rutland (1989). The expression for the circulation Γ, the vorticity ω_z, and the tangential velocity u_θ are expressed in Table 3 in function of the radial coordinate r, the vortex strength Ψ, and the core radius
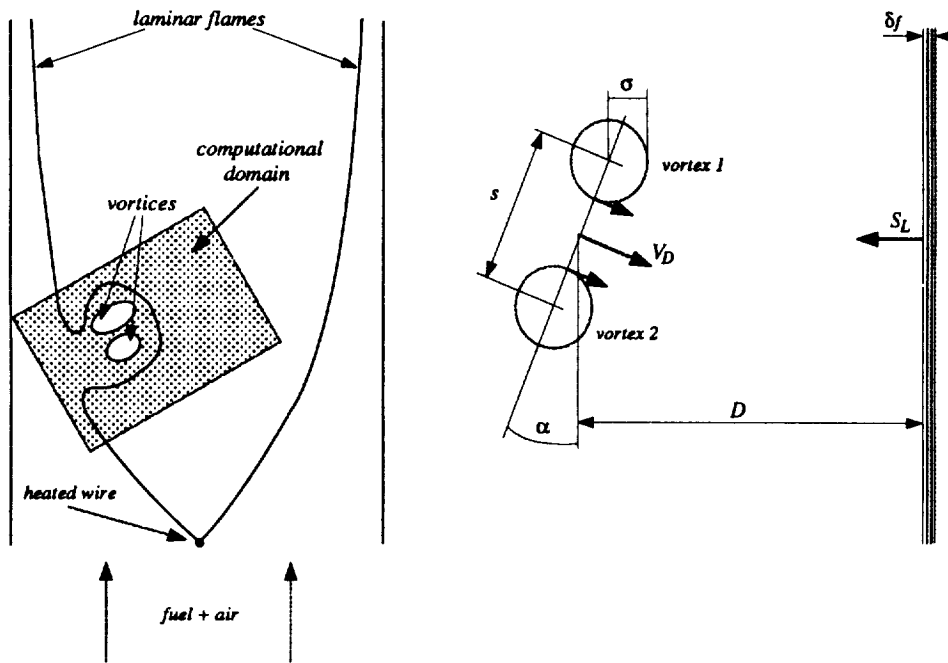
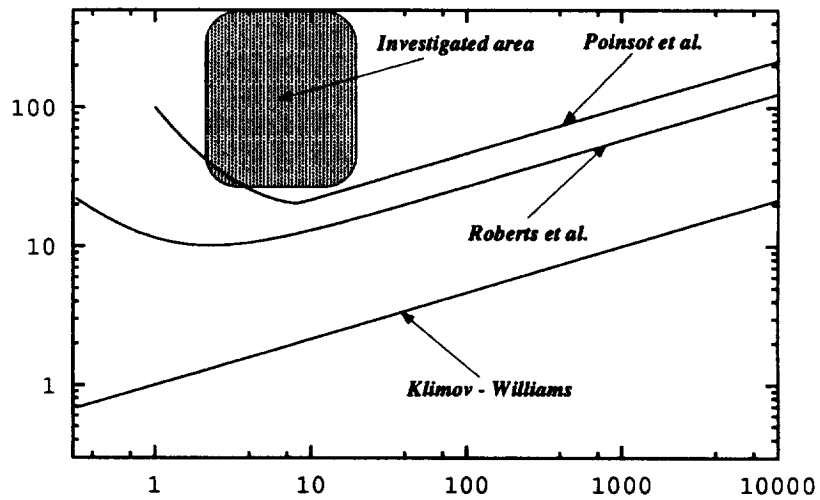FIGURE 1.   Schematic description of the configuration

FIGURE 2.   Diagram of vortex-flame interactions

		vortex 1		*vortex 2*					
Le	case	$\Gamma_1/S_L^0\delta_f$	Re_1	$\Gamma_2/S_L^0\delta_f$	Re_2	s/δ_f	D/δ_f	V_D/S_L	Da
1.0	1	3286	4600	3569	5000	36.5	104.8	14.9	1.9
	2	5657	8000	6686	9333	25.7	104.8	38.1	0.53
	3	10286	14667	11314	16000	25.7	104.8	66.8	0.3
1.8	1	3286	4600	3571	5000	40.5	104.8	13.5	2.91
	2	5714	8000	6667	9333	28.6	104.8	34.5	0.81
	3	10476	14667	11428	16000	28.6	104.8	61.0	0.45

Table 2. Dimensionless parameters for each configuration

vortex "hat"	*Oseen vortex*
$\Gamma = 2\pi\Psi\dfrac{r^2}{\sigma^2}\exp(-\dfrac{r^2}{\sigma^2})$	$\Gamma = \Psi(1 - \exp(-\dfrac{r^2}{\sigma^2}))$
$\omega_z = \dfrac{\Psi}{\sigma^2}(2 - \dfrac{r^2}{\sigma^2})\exp(-\dfrac{r^2}{2\sigma^2})$	$\omega_z = \dfrac{\Psi}{\pi\sigma^2}\exp(-\dfrac{r^2}{\sigma^2})$
$u_\theta = \dfrac{\Psi r}{\sigma^2}\exp(-\dfrac{r^2}{2\sigma^2})$	$u_\theta = \dfrac{\Psi}{2\pi r}(1 - \exp(-\dfrac{r^2}{\sigma^2}))$

Table 3. Circulation Γ, vorticity ω_z, and tangential velocity u_θ for the vortex "hat" and the Oseen vortex

σ. The distribution of these quantities for the Oseen vortex and for the vortex "hat" are schematically represented in Fig. 3.

Because its compact structure allows us to avoid numerical difficulties related to the boundaries of the domain (and then to reduce the size of the computational box), the vortex "hat" has been utilized in several studies (Rutland & Ferziger 1991, Poinsot et al. 1991). However, the vortex "hat" exhibits a rapid decrease of the tangential velocity and an inversion of the sign of the vorticity for $r = \sqrt{2}\sigma$, which is not representative of real vortices. During the interaction with the flame, this opposite vorticity generates undesirable stretch, leading to an artificial increase of the flame length. To avoid these problems and to perform future quantitative comparison with the experimental results of Samaniégo et al. (1994), the Oseen
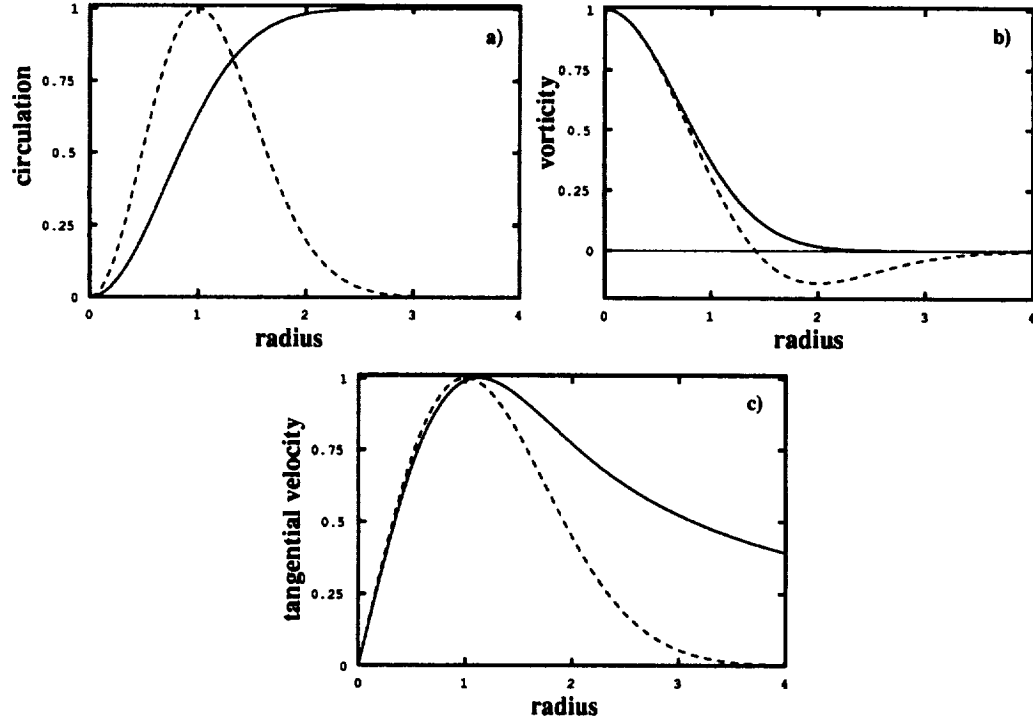
FIGURE 3.   Characteristics of the vortices a) circulation Γ, b) vorticity ω_z, c)
tangential velocity u_θ; ———— : Oseen vortex; ········ : "hat vortex".

vortex is utilized in all our simulations.

For these two-dimensional simulations, the computational domain is typically
composed by 300000 grid points (750 × 400).

2.1.7 Remarks

In the simulations, some parameters have to be treated carefully in order to
perform quantitative comparisons with the experiment. The interaction between the
vortex pair and the flame can be entirely defined by the following set of parameters:

- the ratio between the displacement velocity of the vortex pair and the laminar
  flame speed V_D/S_L;

- the ratio between the distance separating the center of the vortices and the
  laminar flame thickness s/δ_f;

- the distance D separating the vortex pair and the flame;

- the temperature jump across the flame front represented by the heat release
  parameter α;

- the activation energy of the chemical reaction(s) represented by the Zel'dovich
  number(s) $\beta_{(k)}$;

- the ratio between the frequency factors Λ_2/Λ_1 for the two-step mechanism.

Although it sets the laminar flame velocity, the frequency factor Λ for the one-step chemical model (and Λ_1 for the two-step mechanism) is not a determining parameter in this study. Indeed, the laminar flame velocity can be chosen arbitrarily as long as the ratio V_D/S_L is appropriate and the effects related to the compressibility of the flow are avoided. The only restriction is to limit the Mach number, based on the maximum velocity present in the flow field, to be below a critical value (i.e. 0.2). This restriction has an important practical impact, because it considerably reduces the computational time of the simulations.

As we have already mentioned, the experiment allows us to determine the individual circulation of the vortices and the distance separating the center of the vortices, the radius of the viscous core σ and the exact distribution of the tangential velocity being unknown. However, the information provided by the experiment is enough to give a good representation of the interaction. Vortex pairs propagate by mutual induction, and, for point vortices, the displacement velocity of the ensemble is defined by the circulation of the vortices Γ and the distance separating the vortices s (Prandtl & Tietjens 1934):

$$V_D = \frac{\Gamma}{2\pi s} \tag{2.25}$$

Although in the experiment the vortex cores definitely have a finite radius, some simulations performed on simple cases show that as long as the circulation of each of the vortices is conserved and the radius of the viscous cores is restricted to $0 < \sigma/s < 1/2$, the dynamics of the interaction and the strain field applied to the flame are the same. Thus, in all the simulations presented here, the ratio σ/s is set to $1/3$.

In other words, for given circulation Γ and distance s, vortex flame interactions can be represented either by point vortices or by finite viscous core radius and lead to the same conclusions. This last point has a very important impact on the elaboration of combustion diagrams for vortex flame interactions proposed by Poinsot *et al.* (1991) usually defined by u_θ^{max}/S_L and σ/δ_f. Thus, using the characteristics of the Oseen vortex reported on Table 3, a vortex flame interaction can be represented in the diagram by an infinity of points related by the relation:

$$\frac{u_\theta^{max}}{S_L} = \frac{Re_v}{2\pi} Pr \left(\frac{\sigma}{\delta_f} \right)^{-1} \tag{2.26}$$

where $Re_v = \Gamma/\nu$ is the Reynolds number of the vortex. Here, we propose to use the parameters V_D/S_L and s/δ_f to classify vortex flame interactions in the diagram of Poinsot *et al.* (1991). Note that, since the ratios u_θ^{max}/V_D and σ/s in Poinsot *et al.* (1991) and Roberts *et al.* (1993) are not far from unity, the conclusions of their study are still valid and are not contradicted by our comments.

2.1.8 Post processing

The experimental results obtained by Samaniego *et al.* (1994) concern essentially the CH emission of the flame during the interaction. The CH emission of the flame is directly related to the heat release rate of the flame, as shown by the numerical
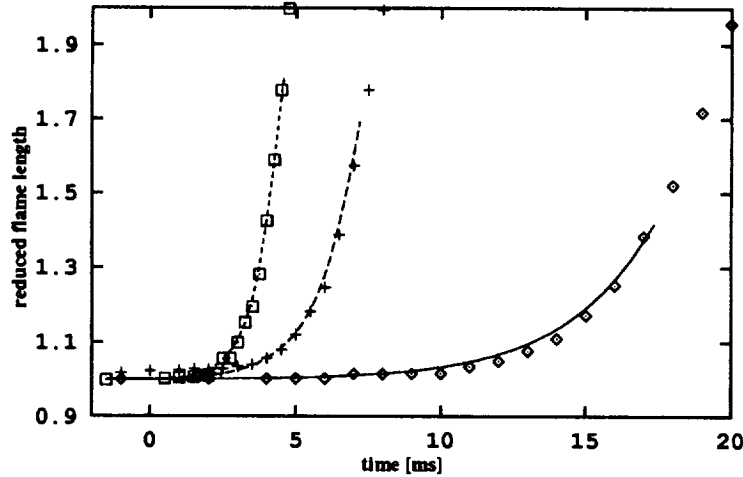
FIGURE 4.   Evolution in time of the reduced flame length Σ^* ; Case 1: —— : DNS, $\diamond$: exp ; Case 2: – – – : DNS, + : exp ; Case 3: ······ : DNS, □ : exp

analysis of Samaniégo (1994). Samaniego *et al.* relate the light emission of a strained laminar methane-air flame I_{CH_4} and the light emission of a strained laminar propane-air flame $I_{C_3H_8}$ to the heat release rate RR according to the following power laws:

$$RR = I_{CH_4}^{0.37} \tag{2.27}$$

$$RR = I_{C_3H_8}^{0.63} \tag{2.28}$$

Thus, quantitative comparisons will be performed accurately both for methane-air and propane-air flames.

In this section, local characteristics of the flame such as the tangential strain, the curvature, the normal towards the fresh gases, and the flame length Σ are obtained at the flame front location $Y_A/Y_{A_u} = 0.2$ where Y_A represents the mass fraction of the reactant A.

2.2 Results

In the first part of this section, the results are presented for simulations performed with the one-step chemical model. In this model, the heat release parameter α is set to 0.8 and the Zel'dovich number β to 8.0, corresponding to an activation energy of 30 kcal/mol.

Before discussing in more detail the physical effects affecting the local structure of the flame during the interaction, the evolution in time of the reduced flame length $\Sigma^* = \Sigma/\Sigma_0$ for $Le = 1.0$ and the three interactions shown in Table 2 are presented in Fig. 4.

The comparison with the experimental results of Samaniego *et al.* (1994) points out that the dynamics of the interactions is very well reproduced by the simulation. This enhances the reasonable approximations made concerning the internal structure of the vortices and their initialization.
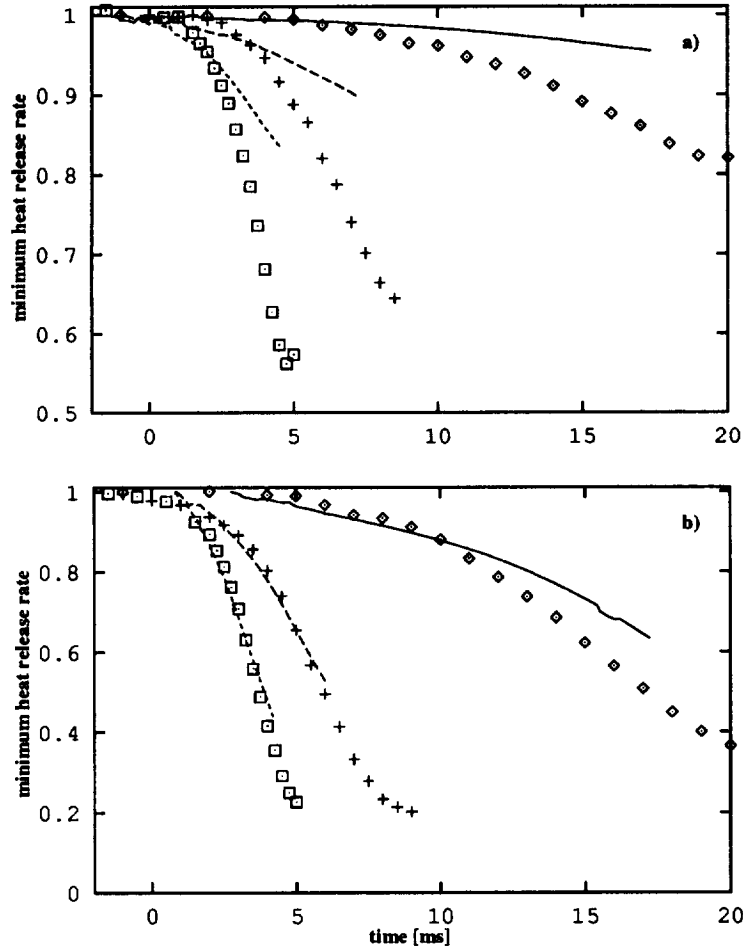
FIGURE 5. Evolution in time of the minimum heat release rate. a) $Le = 1.0$; b) $Le = 1.8$ Case 1: ——— : DNS, ◇ : exp; Case 2: ———— : DNS, + : exp; Case 3: —————— : DNS, ▫ : exp

Fig. 5 describes the time evolution of the minimum of the heat release rate along the flame front for the different interactions presented in Table 2. For $Le = 1.0$ (Fig. 5-a), the agreement is poor between the simulations and the experiment even if the sensitivity to the Damköhler number is qualitatively represented by the DNS. For $Le = 1.8$ (corresponding to the propane-air flame), the simulations seem to well reproduce the decrease of the minimum heat release rate for the three interactions, especially those corresponding to low Damköhler numbers.

The same comments can be made concerning the distribution of the heat release rate along the flame front where the simulations greatly overestimate the heat release for $Le = 1.0$ (see Fig. 6), whereas the agreement is notably better for $Le = 1.8$ (see Fig. 7).

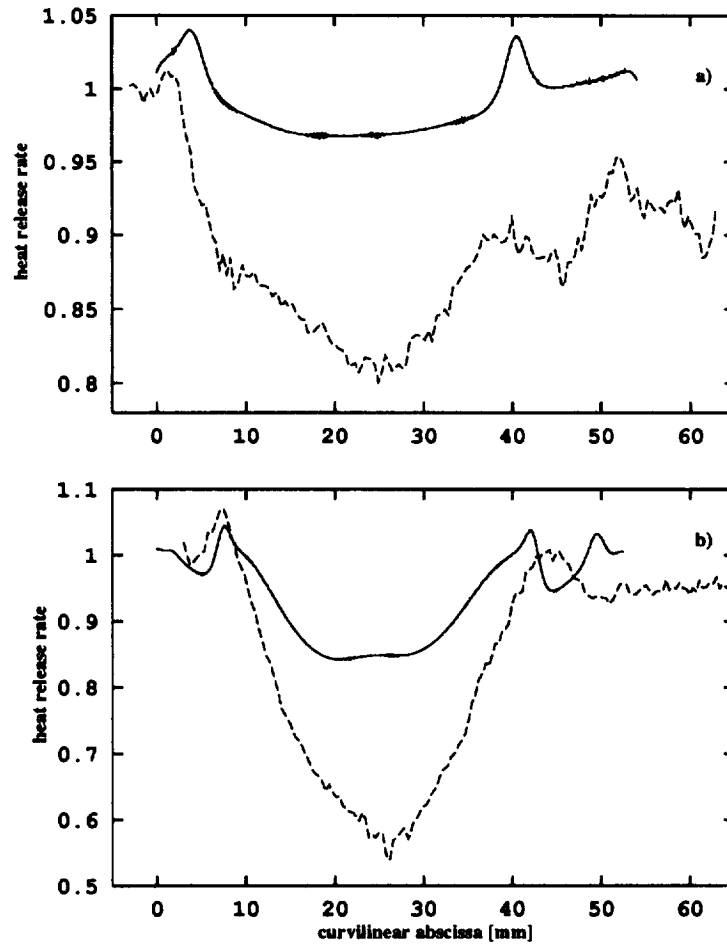For $Le = 1.8$, the Lewis number effect alone can explain the decrease of the heat

FIGURE 6. Distribution of the heat release rate along the flame front. $Le = 1.0$;
a): case 1, b): case 3 ; ——— : DNS, ---- : exp

release rate during the interaction and seems to be the parameter controlling the
local structure of the flame. However, the simulations presented here are performed
for an adiabatic flame using a one-step chemical model. Thus, phenomena such
as radiative heat losses and complex chemistry effects are not taken into account
and could have a significant impact on the interaction, which could explain the
discrepancies found between the DNS and the experiment, especially for $Le = 1.0$.

In the following sections, the contributions of the major physical effects suspected
of playing a role in the mechanism of extinction (stretch, heat losses, complex
chemistry) and responsible for the decrease of the heat release rate observed during
the interaction will be analyzed in detail.

2.2.1 Analysis of the stretch

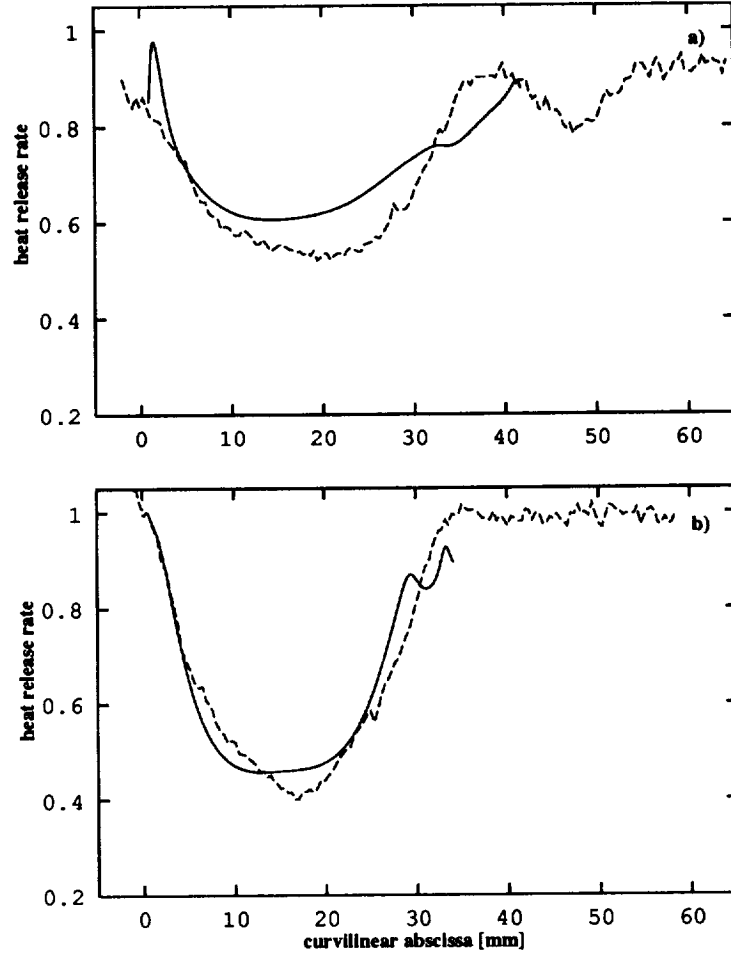In the configuration studied here, the flame is subjected to curvature and straining

FIGURE 7. Distribution of the heat release rate along the flame front
$Le = 1.8$; a): case 1, b): case 3 ; ———— : DNS, - - - - : exp

effects, causing a modification of the flame length. These changes imposed on the flame can be estimated from the flame stretch κ. From Williams (1985), κ is defined by the rate of change of a Lagrangian flame surface element A:

$$\kappa = \frac{1}{A}\frac{dA}{dt}$$ (2.29)

This expression can be rewritten in terms of flame stretch and flame curvature (Matalon 1983, Candel & Poinsot 1990):

$$\kappa = \mathbf{nn} : \nabla\mathbf{w} + \nabla.\mathbf{w}$$ (2.30)

where **n** is the unit vector normal to the flame surface pointing towards the fresh gases:

$$\mathbf{n} = -\frac{\nabla c}{|\nabla c|}$$ (2.31)

and **w** is the local velocity of the flame surface. In indicial notation, **nn** : $\nabla \mathbf{w} = n_i n_j \partial w_i / \partial x_j$. The local flame front velocity can be decomposed in a convective velocity in the fresh gases **u** and a displacement speed S_d (see Poinsot *et al.* 1992). Thus, expression 2.30 becomes:

$$\kappa = \nabla_t . \mathbf{u} - \frac{S_d}{\mathcal{R}} \tag{2.32}$$

where $\nabla_t . \mathbf{u}$ represents the strain contribution and $S_d / \mathcal{R}$ the curvature term ($\mathcal{R}$ is the local radius of curvature of the flame front).

As it has been shown by Poinsot *et al.* (1992), the displacement speed S_d is not equal to the laminar flame speed S_L and can be significantly different. The displacement speed can be exactly determined by solving the equation for an iso-contour $c = c_0$ (which is nothing but the G-equation described in Kerstein *et al.* 1988) as it has been proposed by Trouvé & Poinsot (1994). The equation for an iso-scalar surface $c = c_0$ is written:

$$\frac{\partial c}{\partial t} + \mathbf{w} . \nabla c = 0 \tag{2.33}$$

Utilizing Eq. 2.30 in Eq. 2.32 and noting that $S_d = \mathbf{w} . \mathbf{n} - \mathbf{u} . \mathbf{n}$, an expression for S_d can be derived:

$$S_d = \frac{1}{|\nabla c|} \left(\frac{\partial c}{\partial t} + \mathbf{u} . \nabla c \right) \tag{2.34}$$

Fig. 8 represents the relative contribution of strain and curvature on the stretch along the flame front for case 3 of Table 2 at the end of the interaction ($t = 3.3$ms).

One sees that the maximum stretch does not appear on the trajectory described by the ensemble as it could be expected. The maximum of stretch occurs on both sides of this trajectory corresponding to each of the vortices. This feature was also observed by Driscoll *et al.* (1994) in their PIV measurements.

As expected due to the size of the vortex pair compared to the flame thickness, the contribution of the curvature on the global stretch is very weak (about a few percent) compared to the contribution of the tangential strain, especially in regions where a significant decrease of the heat release rate is observed. This corroborates the conclusions of Driscoll *et al.* (1994), who performed a measurement of the velocity field during vortex-flame interaction using a PIV technique. We can also see that the levels of strain rate reached during the interaction are extremely high compared to the extinction strain rate measured for steady counterflowing premixed flames (Law *et al.* 1986, Tsuji & Yamaoka 1982) and for the vortex-flame interaction of Driscoll *et al.* (1994). In Tsuji & Yamaoka (1982), the extinction strain rate of a methane-air flame with an equivalence ratio of 0.52 is only $42 s^{-1}$. During the interaction of ring vortices and a premixed methane-air flame with an equivalence ratio of 0.55, the extinction strain rate measured by Driscoll *et al.* (1994) is $35 s^{-1}$ and corresponds to a Karlovitz number of 0.12. In the present interactions, the Karlovitz number reaches higher values up to 3.0 (see Fig. 9).

Apparently, the configuration retained in our study exhibits a very resistant flame compared to the steady situations of Tsuji & Yamaoka (1982) and particularly compared to the ring vortices-flame interaction of Driscoll *et al.* (1994). In this last study, local quenching is clearly observed during the interaction. On the contrary in our study (both in the experiment and in the simulations), all the cases investigated here are far from the quenching limit encountered by Roberts *et al.* (1993) and by Driscoll *et al.* (1994). In all our simulations, the minimum heat release rate never decreases under 30% of the heat release rate corresponding to an unstrained laminar flame (see Fig. 5). Moreover, we observe that it is more difficult to quench a methane-air flame having a Lewis number of unity rather than a propane-air flame with $Le = 1.8$. These conclusions are in accordance with the classical analytical results concerning the theory of stretched flames (Clavin & Williams 1982, Clavin 1985, Law 1988) and also with the experimental results of Law *et al.* (1986), but are in contradiction with the observations of Roberts *et al.* (1993).

For $Le = 1.0$, we observe a good correlation between the strain rate and the local flame speed with a slight negative slope [1] (see Fig. 10-a). This is due to the compression of the reaction zone by the local extensive strain. This observation is consistent with the results of Haworth & Poinsot (1992) and is illustrated in Fig. 11, which shows the scatter plot of the thermal flame thickness $\delta_T^* = \delta_T/\delta_T^{uns}$ (based on the maximum temperature gradient) versus the local flame speed. A very good correlation is found between δ_T^* and S_L^* and clearly shows a compression of the flame (down to 70% for the higher strain rates) corresponding to low values of S_L^*. Conversely, a thickening of the flame (up to 10%) corresponds to higher flame velocities and regions of compression of the flame.

For $Le = 1.8$ (see Fig.10-b), the correlation between S_L^* and Ka is less obvious even if we observe a clear decrease of the local flamelet velocity for positive stretch as it can be expected for strained laminar flame having a Lewis number greater than unity.

2.2.2 Effect of the radiative heat losses

Radiative heat losses occurring in the burnt gases of a premixed laminar flame produce a natural decay of the temperature and have been suspected of being partially or totally responsible for quenching during vortex-flame interaction (Poinsot *et al.* 1991, Roberts *et al.* 1993). In their numerical study (and using a one-step mechanism for the chemistry), Poinsot *et al.* (1991) concluded that stretch alone cannot be responsible for quenching. Local extinction occurs only when stretch and radiative heat losses present in the burnt gases are combined. The authors observed that during the quenching process, pockets of fresh gases can be present in the burnt gases and cannot reignite due to a too low temperature. However, in order to obtain such behavior, very high (and unrealistic) heat losses have been imposed to the flame. In comparison, we will see that the heat losses measured by Roberts *et al.* (1993) and by Samaniego *et al.* (1994) are lower by an order of magnitude than in

---

[1] The local flame speed is calculated by integrating the reaction rate in a direction normal to the flame front: $S_L = \frac{1}{\rho_u Y_{A_u}} \int_{-\infty}^{\infty} \dot{w} \, dn$
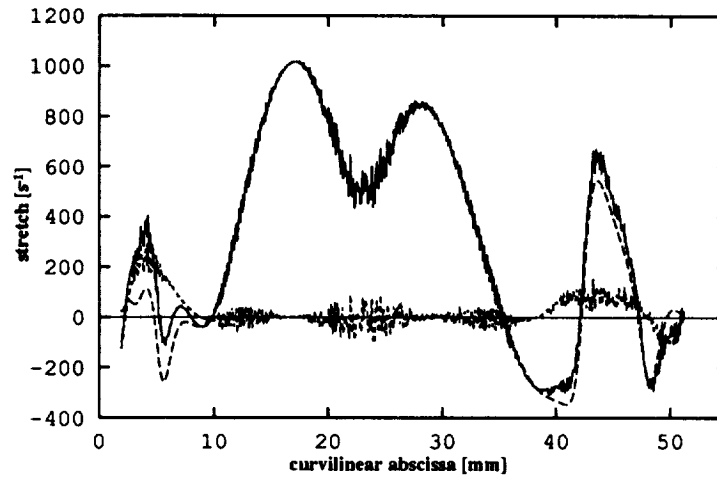
FIGURE 8. Contribution of tangential strain and curvature on stretch, Case 3
$Le = 1.0$; ——— : total stretch, - - - - : curvature, - - - - - : tangential strain
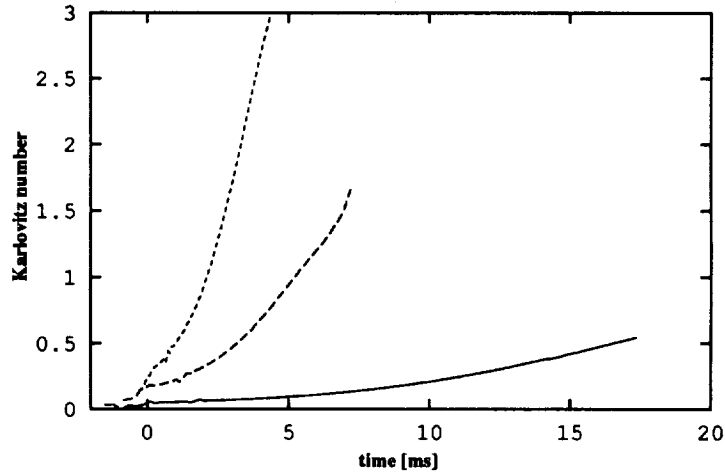

FIGURE 9. Evolution in time of the Karlovitz number for Le = 1.0
——— : case 1, - - - - : case 2, - - - - - : case 3

Poinsot *et al.* (1991). Since in their simulations a single-step mechanism has been used, it is still not clear if quenching in real flames is due to combined stretch and heat loss effects, or to combined stretch and complex chemistry effects.

Here, in order to quantify the impact of realistic heat losses on the distribution of the reaction rate along the flame front, a simulation corresponding to the interaction 2 of Table 2 for $Le = 1.0$ is performed. Different levels of heat loss corresponding to the experiments of Roberts *et al.* (1993) and Samaniego *et al.* (1994) and to the numerical study of Poinsot *et al.* (1991) are investigated. Before discussing the results of these simulations, the quenching limit of a one-dimensional non-adiabatic
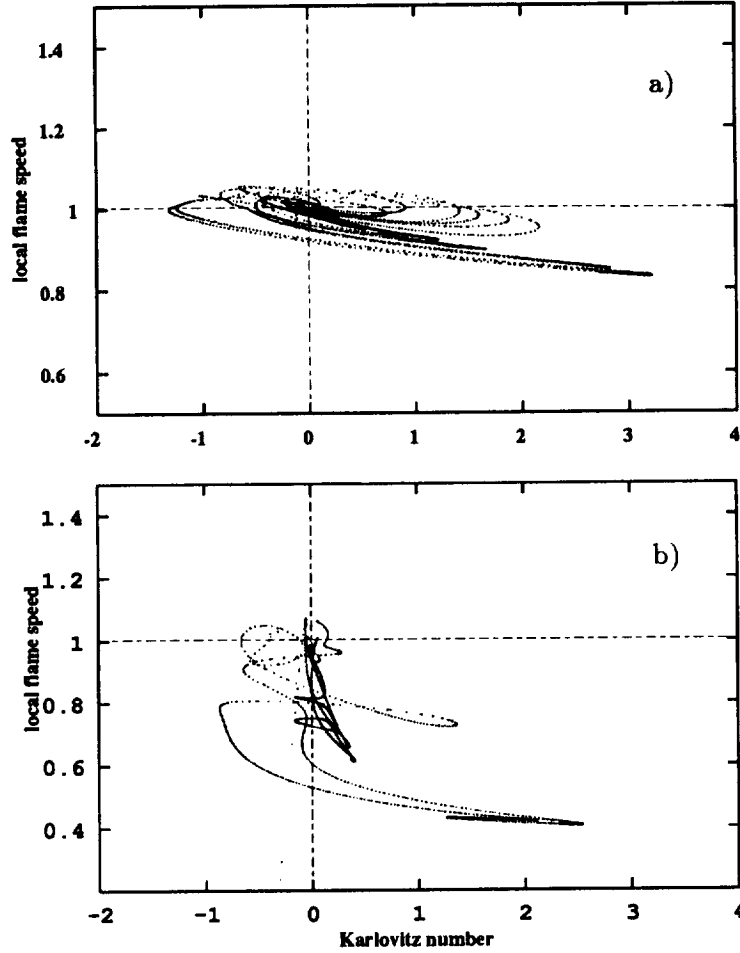
FIGURE 10. Scatter plot of local flame speed versus Karlovitz number,
a): $Le = 1.0$; b): $Le = 1.8$

flame is investigated. This analysis should allow us to recover the asymptotic solution of Williams (1985), who proposes an analytical relation between the laminar flame velocity and the heat loss parameter. This relation is expressed (Williams 1985 p. 275):

$$\xi^2 = \exp\left(-\frac{l}{\xi^2}\right) \tag{2.34}$$

where $\xi = S_L/S_L^{ad}$. From this relation, the quenching limit corresponds to $l = 1/e$ leading to a reduced laminar burning velocity $\xi = 1/\sqrt{e}$.

Fig. 12 shows the evolution of the burning velocity ratio ξ versus the heat loss parameter l given by the simulation and by the relation 2.34 for two different Zel'dovich numbers ($\beta = 8$ and $\beta = 16$). A very good agreement is found between the simulations and the asymptotic theory of Williams, especially for very large activation
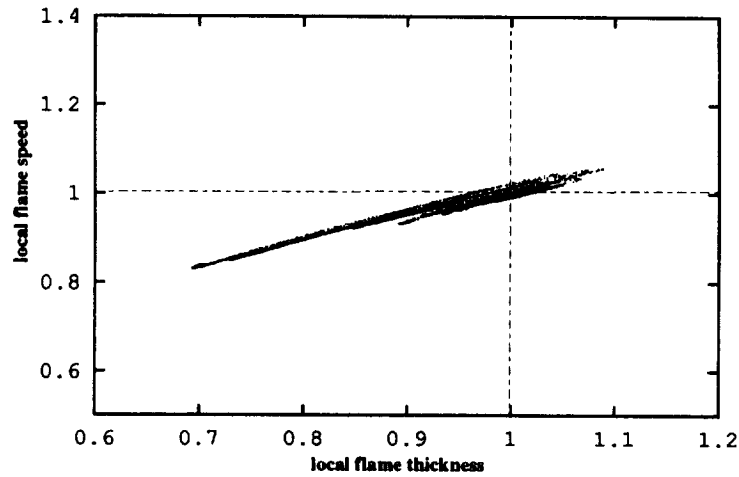
FIGURE 11.   Scatter plot of local flame speed versus the reduced local flame thickness
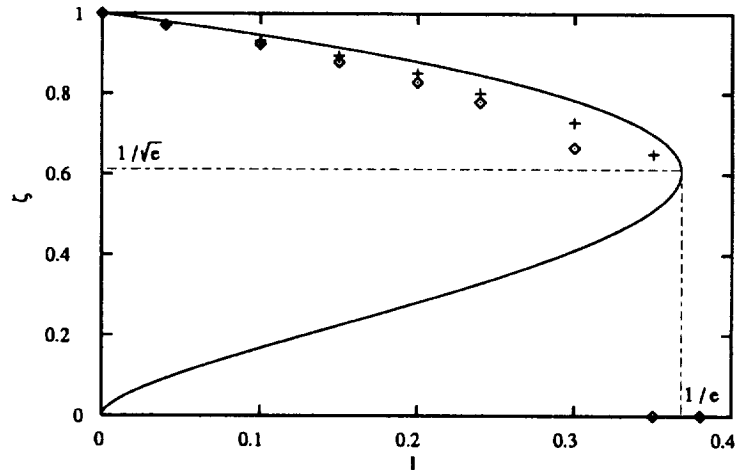

FIGURE 12. Burning velocity ratio versus heat loss parameter ; ——— asymptotic theory, ◇ : $\beta = 8.0$, + : $\beta = 16.0$

energy.

In the simulation corresponding to the case 2 for $Le = 1.0$, various values for the heat loss parameter l are investigated. The case $l = 0$ corresponds to the adiabatic case, $l = 0.008$ and $l = 0.027$ to the heat losses estimated from the experiment of Samaniégo *et al.* (1994) and from Roberts *et al.* (1993). The case $l = 0.3$ represents the heat losses used by Poinsot *et al.* (1991). According to Fig. 12, only a negligible effect of radiative heat losses is expected to be found in Samaniégo *et al.* (1994) and in Roberts *et al.* (1992). Nevertheless, the effect should be much more pronounced for the heat losses of Poinsot *et al.* (1991) which are close to the
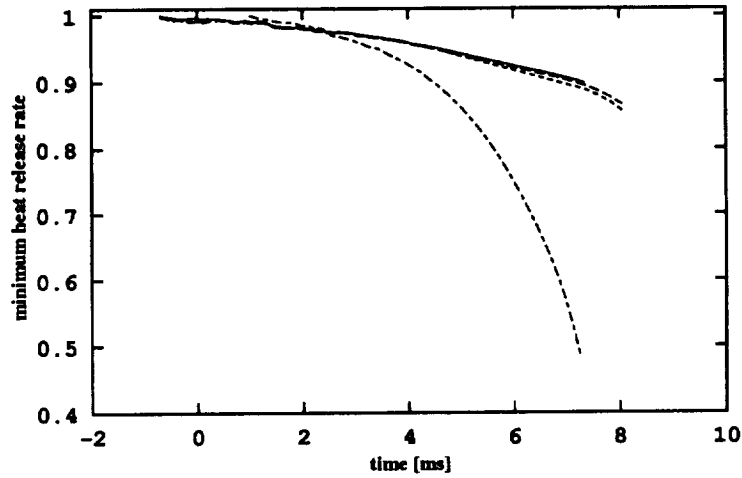
FIGURE 13. Evolution in time of the minimum heat release rate, case 2 $Le = 1.0$; —— adiabatic, ———— : $l = 0.008$, ------ : $l = 0.027$, ———— : $l = 0.3$.

quenching limit observed for a one-dimensional unstrained non-adiabatic laminar flame. Fig. 13 represents the time history of the minimum heat release encountered along the flame front. As expected, the heat losses found in the two experiments have a negligible effect on the evolution of the heat release rate. On the other hand, very intense heat losses (more representative of conductive heat losses to a wall) can lead to a dramatic decrease of the heat release and to probable local quenching even if the computation does not go sufficiently far in the interaction to clearly show it.

These simulations are performed using a one-step chemical model and do not take into account combined effects of radiative heat losses and complex chemistry. These combined effects can have a significant influence on the flame structure when the flame is close to its flammability limits, as illustrated by the numerical study of Egolfopoulos (1994). The author investigates the response of a lean methane-air flame submitted to stretch and radiative heat losses using the GRI (Gaz Research Institute) mechanism. For a laminar methane-air flame with an equivalence ratio of 0.55, Fig. 14 shows the evolution of the reduced heat release $\dot{Q}/\dot{Q}_0^{ad}$ as a function of the tangential strain. Results for the adiabatic and non-adiabatic cases are presented. We can observe that the heat release rate is strongly influenced by the heat losses for the unstrained laminar flame and decreases down to 0.83. For high values of the strain (typically those encountered in our configuration), the effect of the radiative heat losses compared to the effect of the strain on the decrease of $\dot{Q}/\dot{Q}_0^{ad}$ is much weaker.

2.2.3 Role of an intermediate species in strained laminar flames

The chemistry of simple hydrocarbons such as methane can be described by full mechanisms available in the literature (Westbrook & Dryer 1984, Miller & Bowman 1989). The coupling of these mechanisms with a DNS code has been performed by Baum *et al.* (1992) but leads to extremely high computational time. As an
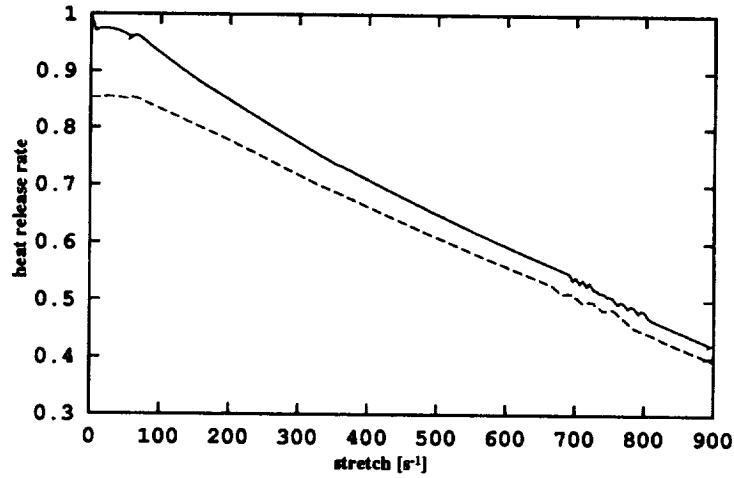
FIGURE 14. variation of the heat release rate versus stretch for a one-dimensional premixed strained flame (from Egolfopoulos 1994) ———— : adiabatic , ———— : non-adiabatic

alternate possibility, reduced chemical schemes for the combustion of methane-air flames (Peters & Williams 1987) and for propane-air flames as well (Kennel *et al.* 1990) exist and can be used in DNS codes.

Here, a two-step mechanism described by a first chain branching step $A + X \rightarrow 2X$ and a second chain terminating step $X + X \rightarrow P$ is utilized to analyze the structure of the flame during its interaction with a vortex pair.

In the asymptotic analysis of a premixed laminar flame submitted to stretch, Seshadry & Peters 1983 have put into evidence the role played by the radical species on the flame structure (see §2.1.3).

Since the Lewis number for the intermediate species is less than unity (due to the high diffusivity of the radicals), positive stretch will generate a high diffusion of radicals out of the reaction zone. Thus, the concentration of radicals in the reaction zone will decrease, leading to a lower heat release rate (because of the quadratic dependence on Y_X of the heat release rate, see Eq. 2.14). This behavior is well reproduced by the asymptotic expression for the temperature given by Eq. 2.19.

From the discussion presented in §2.1.3, the set of parameters for the two-step mechanism can entirely be determined by considering the data presented in Table 1 and the temperature of the burnt gases (in the experiment $T_b = 1500K$). This leads to $\Lambda_2/\Lambda_1 = 0.53$, $\beta_1 = 4.83$, $\beta_2 = 0$, and $Le_X = 0.15$ (here using the Lewis number for the H atom).

Fig.15 shows the evolution in time of the minimum heat release rate during the interactions for $Le = 1.0$ and $Le = 1.8$ for the cases 1 and 3 of Table 2. Here, the decrease of $\dot{Q}$ is very well reproduced by the two-step mechanism, regardless of the Damköhler number. This is particularly interesting for the methane-air flame cases for which the one-step mechanism poorly describes the decrease of $\dot{Q}$ (see Fig. 5-a).
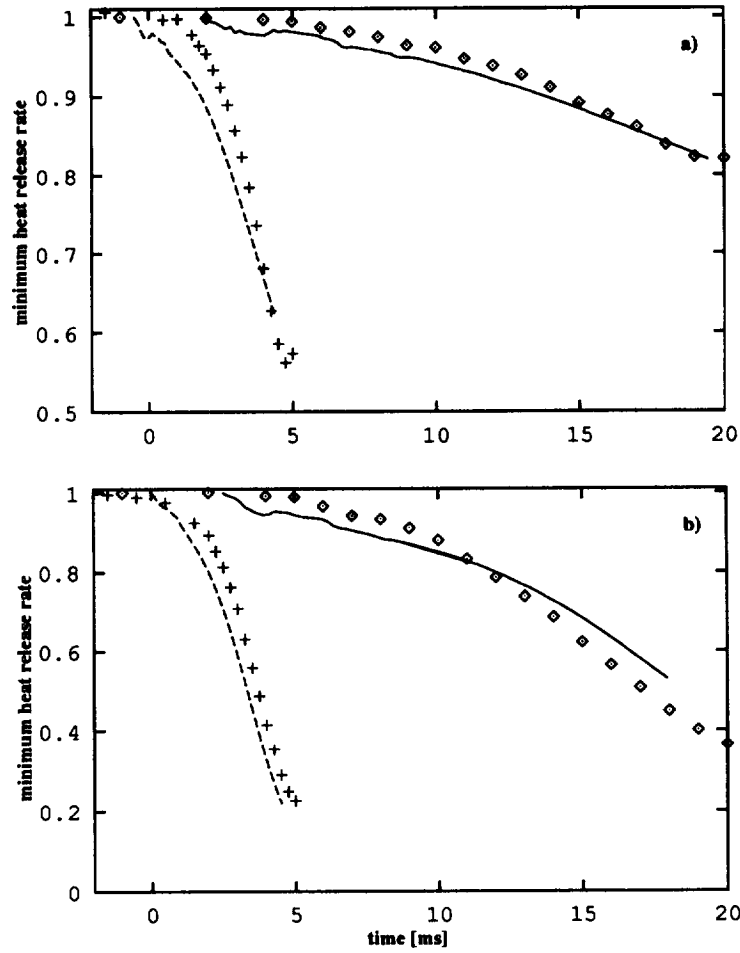
FIGURE 15. Evolution in time of the minimum heat release rate. a) $Le = 1.0$ b) $Le = 1.8$ Case 1: ——— : DNS, ◊ : exp; Case 2: ---- : DNS, + : exp; Case 3: ------ : DNS, □ : exp.

The coherent behavior of the two-step mechanism is confirmed by the distribution of $\dot{Q}$ along the flame front (see Figs. 16 and 17). For $Le = 1.0$, the agreement between the DNS and the experiment is excellent and is greatly improved compared to the results obtained with the one-step mechanism (see Fig. 6). A minor quantitative discrepancy exists in regions of the flame where curvature effects are non-negligible although the tendencies are well reproduced.

The same comment can be made for $Le = 1.8$, where a good agreement is observed for the two Damköhler numbers studied here (Figs. 15-b and 17). However, the two-step mechanism does not significantly improve the results, which are already satisfactory using the one-step model (see Fig.7).

Fig. 18 shows the scatter plot of the local flame speed versus the Karlovitz number. Regions of the flame submitted to positive stretch exhibits a decrease of the local
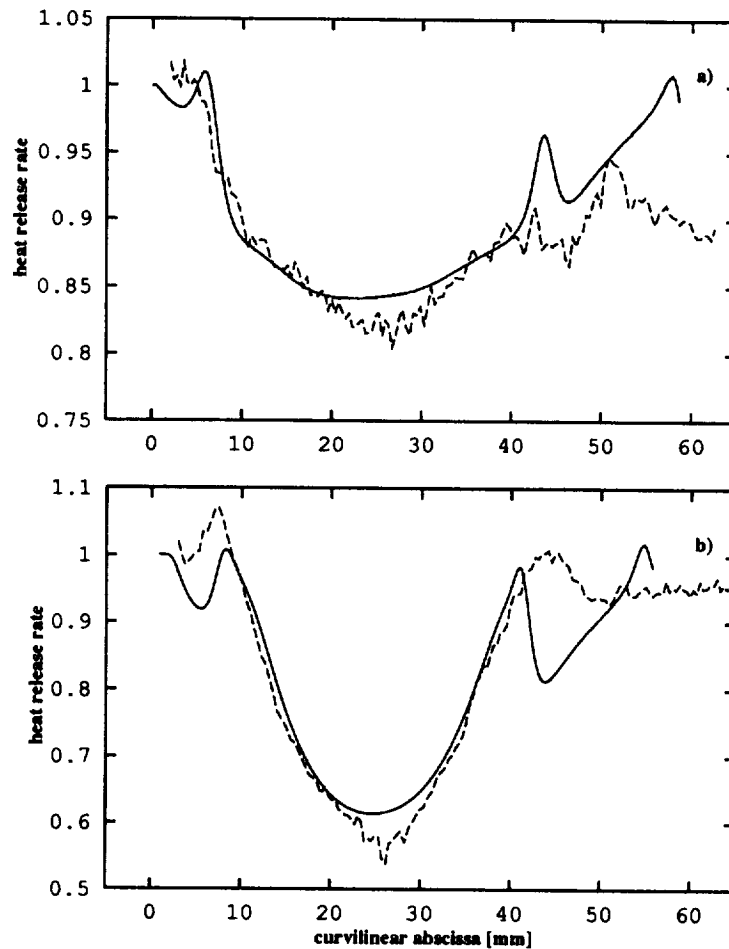
FIGURE 16.   Distribution of the heat release rate along the flame front. $Le = 1.0$;
a): case 1, b): case 3; ———— : DNS, – – – – : exp.

flame speed as it is observed for stretched flames having a Lewis number greater than unity. As a consequence, a flame having a Lewis number of unity described with a two-step mechanism behaves like a laminar flame having an apparent Lewis number greater than unity. This particular point provides evidence for the existence of a critical Lewis number Le_c smaller than unity for which moderate stretch does not affect the flame structure.

According to these observations, the concentration of radicals seems to be the key parameter which controls the local flame structure and quenching mechanism. This has been shown by the asymptotic analysis on the structure of strained premixed flames by Seshadry & Peters (1983) and is confirmed in the present study. Moreover, the quenching of a premixed laminar flame propagating toward a cold wall is also strongly dependent on the concentration of radicals (Hocks *et al.* 1981).

However, it is difficult to separate which parameter of the two-step mechanism
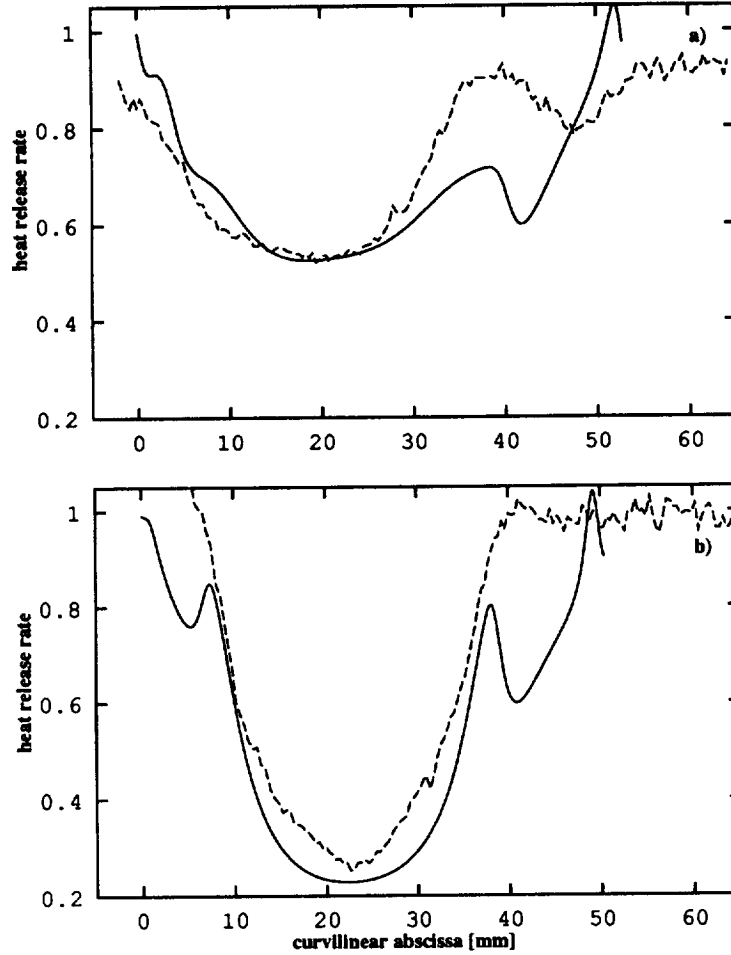
FIGURE 17. Distribution of the heat release rate along the flame front. $Le = 1.8$; a): case 1, b): case 3; ——— : DNS, ———— : exp.

is predominant (ratio Λ_2/Λ_1, Lewis number for the intermediate species, activation energy for the first and second step). For instance, to describe the flame quenching at a wall, Hocks *et al.* (1981) have considered a low recombination regime, a high activation energy for the first reaction, and equal diffusivities of heat and mass ($\Lambda_2/\Lambda_1 = 5\ 10^{-4}$, $\beta_1 = 8.5$, $\beta_2 = 0$, $Le_X = 1.0$). This choice has been made arbitrarily by the authors and justified by comparing the concentration of radicals given by the two-step mechanism to the concentration of intermediate species such as OH, H, and O given by complex chemistry calculations of the same configuration. Here, the choice of the set of parameters is based on physical arguments (justified in §2.1.3), which seems to be reasonable if we consider the agreement between the DNS and the experiment for all the cases studied here. The two-step mechanism shows its ability to describe vortex-flame interactions on a large range of Damköhler number (0.3 to 2.9).
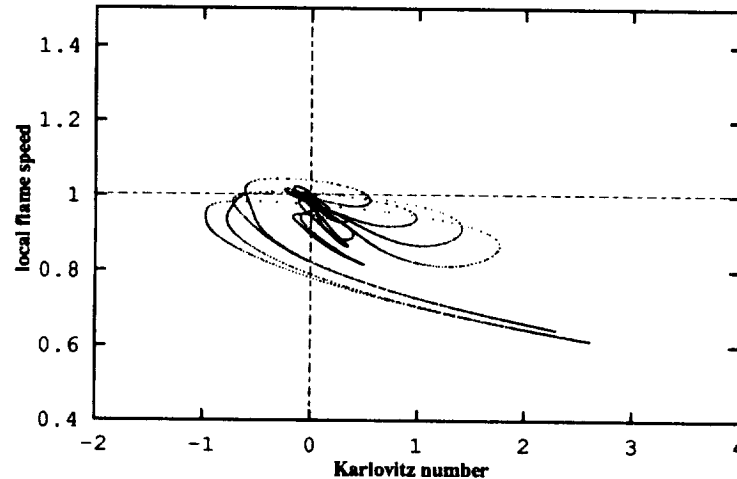
FIGURE 18. Scatter plot of local flame speed versus the Karlovitz number.

Conclusion

Direct numerical simulations of flame vortex interactions are performed using one-step and two-step chemical models.

Simulations performed with the one-step mechanism exhibit a strong disagreement between the DNS and the experiment for all the interactions with $Le = 1.0$. The simulations greatly overestimate the distribution of the heat release rate along the flame front during the interaction. On the contrary, for $Le = 1.8$, the agreement between the simulations and the experimental results is satisfactory for all the interactions corresponding to large range of Damköhler numbers (0.3 to 2.9).

- The analysis of the stretch shows a negligible contribution of the curvature due to the large size of the vortex pair compared to the laminar flame thickness. The tangential strain generated by the vortices is responsible for the stretch felt by the flame.

- Radiative heat losses representative of those encountered in the experiment have no effect on the local flame structure. However, tremendous heat losses (more representative of heat losses by conduction to a cold wall) have a dramatic effect on the heat release and lead to local quenching.

- For the two-step mechanism, the set of parameters is entirely determined by considering the rate coefficients of the chain branching reaction $H + O_2 \rightarrow OH + O$ and the terminating reaction $H+OH+M \rightarrow H_2O+M$, which are the most important chain branching and chain breaking reactions of the $H_2 - O_2$ submechanism occurring in the chemistry of hydrocarbons. All the simulations performed with this model (for both $Le = 1.0$ and $Le = 1.8$) lead to very good agreement with the experimental results. During the interaction between the flame and the vortex pair, the concentration of radicals seems to be the key parameter controlling the local structure and the quenching mechanism.

As a consequence, it appears that the two-step mechanism with the set of parameters chosen here is sufficient to describe all the interactions performed experimentally by Samaniégo *et al.* (1994-b).

Since most of the phenomena encountered in these interactions are also present in turbulent premixed flames, it is tempting to extrapolate these conclusions to a general description of turbulent premixed flames.

Acknowledgements

The author would like to thank Professor C. T. Bowman from the Stanford High Temperature Gasdynamic Laboratory for his helpful suggestions concerning the two-step mechanism and Dr. T. Poinsot from CERFACS (France) for his support and his numerous comments. I would specially thank Dr. G. Ruetsch for his valuable help in the implementation of the two-step mechanism and for his constant support and Dr. J.-M. Samaniégo for his perspicacious suggestions and for the innumerable discussions we had during the course of this study.

REFERENCES

BAUM, M., POINSOT, T. J . & HAWORTH, D. C. 1992 Numerical Simulations of Turbulent Premixed $H_2/O_2/N_2$ Flames with Complex Chemistry. *Proc. of the 1992 Summer Program.* CTR, NASA Ames/Stanford Univ. 345-366.

CANDEL, S. M. & POINSOT, T. J. 1990 Flame Stretch and the Balance Equation for the Flame Area. *Combust. Sci. and Tech..* **70**, 1-15.

CLAVIN, P. 1985 Dynamic Behaviour of Premixed Flame Fronts in Laminar and Turbulent Flows. *Prog. Energy Combust. Sci.* **11**, 1-59.

CLAVIN, P. & WILLIAMS, F. A. 1982 Effects of Molecular Diffusion and of Thermal expansion on the Structure and Dynamics of Premixed Flames in Turbulent Flows of Large Scales and Low Intensities. *J. Fluid Mech.* **116**, 251-282.

DRISCOLL, J. F., SUTKUS, D. J., ROBERTS, W. L., POST, M. E. & GOSS, L. P. 1994 The Strain Exerted by a Vortex on a Flame Determined from Velocity Fields Images. *Combust. Sci. and Tech.* **96**, 213-229.

EGOLFOPOULOS, F. N. 1994 Geometric and Radiation Effects on Steady and Unsteady Strained Laminar Flames. *Twenty-Fifth Symposium (International) on Combustion.*

EL TAHRY, S. H., RUTLAND, C. J. & FERZIGER, J. H. 1991 Structure and Propagation Speeds of Turbulent Premixed Flames - A Numerical Study. *Combust. and Flame.* **83**, 155-173.

GLASSMAN, I. 1987 *Combustion.* Academic Press 2nd Ed.

HAWORTH, D. C & POINSOT, T. J. 1992 Numerical Simulations of Lewis Number Effects in Turbulent Premixed Flames. *244.* **405-436.**

HOCKS, W., PETERS, N. & ADOMEIT, G. 1981 Flame Quenching in Front of a Cold Wall Under Two-Step Kinetics. *Combust. and Flame.* **41**, 157-170.

KEE, R. J., RUPLEY, F. M. & MILLER, J. A. 1989 Chemkin-II: A Fortran Chemical Kinetics Package for the Analysis of Gas Phase Chemical Kinetics. *Report SAND89-8009B* Sandia National Laboratories.

KERSTEIN, A. R., ASHURST, W. T. & WILLIAMS, F. A. 1988 Field Equation for Interface Propagation in an Unsteady Homogeneous Flow Field. *Physical Review.* **A-37-7**, 2728-2731.

LAW, C. K. 1988 Dynamics of Stretched Flames. *Twenty-Second Symposium (International) on Combustion.* 1419-1426.

LAW, C. K. & EGOLFOPOULOS, F. N. 1992 *Twenty-Fourth Symposium (International) on Combustion.* 137-144.

LAW, C. K., ZHU, D. L. & YU, G. 1986 Propagation and Extinction of Stretched Premixed FLames. *Twenty-First Symposium (International) on Combustion.* 1419-1426.

LEE, T. W., LEE, J. G., NYE, D. A. & SANTAVICCA, D. A. 1993 Local Response and Surface Properties of Premixed Flames During Interactions with Karman Vortex Streets. *Combust and Flame.* **94**, 146-160.

LELE, S. K. 1992 Compact Finite Difference Schemes with Spectral-like Resolution. *J. Comp. Phys.* **103**, 16-42.

MATALON, M. 1983 On Flame Stretch. *Combus. Sci. and Tech.* **31**, 169-18.1

MILLER, J. A. & BOWMAN, C. T. 1989 Mechanism and Modelling of Nitrogen Chemistry in Combustion. *Prog. Energy Combust. Sci.* **15**, 287-338.

MILLER, J. A., MITCHELL, R. E. SMOOKE, M. D. & KEE, R. J. 1982 Toward a Comprehensive Chemical Kinetic Mechanism for the Oxydation of Acetylene: Comparison of Model Predictions with Results from Flame and Shock Tube Experiments. *Nineteenth Symposium (International) on Combustion.* 181-196.

OSEEN, C. W. 1911 *Arkiv. Mat. Astron. Fys.* **7**, 1.

PICART, A., BORGHI, R. & CHOLLET, J. P. 1988 Numerical Simulation of Turbulent Reacting Flows. *Comput. and Fluids.* **16-4**, 474-484.

POINSOT, T., ECHEKKI, T. & MUNGAL, M. G. 1992 A Study of Laminar Flame Tip and Implications for Premixed Turbulent Combustion. *Combust. Sci. and Tech.* **81**, 45-73.

POINSOT, T. J., HAWORTH, D. C. & BRUNEAUX, G. 1993 Direct Simulations and Modelling of Flame-Wall Interactions for Premixed Turbulent Combustion. *Combust. and Flame.* **95**, 118-132.

POINSOT, T. J. & LELE, S. K. 1992 Boundary Conditions for Direct Numerical Simulations of Compressible Viscous Flows. *J. Comp. Phys.* **101**, 104-129.

POINSOT, T. J., VEYNANTE, D. & CANDEL, S. M. 1991 Quenching Processes and Premixed Turbulent Combustion Diagrams. *J. Fluid Mech.* **228**, 581-606.

PRANDTL, L. & TIETJENS, O. G. 1934 Fundamentals of Hydro and Aeromechanics. Dover.

ROBERTS, W. L., DRISCOLL, J. F., DRAKE, M. C. & GOSS, L. P. 1993 Images of the Quenching of a Flame by a Vortex to Quantify Regimes of Turbulent Combustion. *Combust. and Flame.* **94**, 58-69.

ROBERTS, W. L., DRISCOLL, J. F., DRAKE, M. C. & RATCLIFFE, J. W. 1992 OH Fluorescence Images of the Quenching of a Premixed Flame during an Interaction with a Vortex. *Twenty-Fourth Symposium (International) on Combustion.* 169-176.

RUTLAND, C. J. 1989 Effects of Strain, Vorticity and Turbulence on Premixed Flames. *PhD Thesis* Stanford University, Thermosciences Div.

RUTLAND, C. J. & FERZIGER, J. H. 1991 Simulation of Flame-Vortex Interactions. *Combust and Flame.* **83**, 343-360.

RUTLAND, C. J., FERZIGER, J. H. & EL TAHRY, S. H. 1990 Full Numerical Simulation and Modelling of Turbulent Premixed Flames. *Twenty-Third Symposium (International) on Combustion.* 621-627.

SAMANIÉGO, J.-M. 1994 Lewis number and Damköhler number effects in vortex-flame interactions. *CTR Research Briefs - 1994*, NASA Ames/Stanford Univ.

SAMANIÉGO, J.-M., MANTEL, T. & BOWMAN, C. T. 1994 Fundamental Mechanisms in Premixed Flame Propagation Via Vortex Flame Interactions - Part I: Experiment. Submitted to J. Fluid Mech.

SESHADRY, K. & PETERS, N. 1983 The influence of stretch on a premixed flame with two-step kinetics.

TSUJI, H. & YAMAOKA, I. 1982 *Nineteenth Symposium (International) on Combustion.* 1533.

TROUVÉ, A. & POINSOT, T. 1994 The Evolution Equation for the Flame Surface Density in Turbulent Premixed Combustion. *J. Fluid Mech.* **278**, 1-31.

WESTBROOK, C. K. & DRYER, F. L. 1984 Chemical Kinetic Modeling of Hydrocarbon Combustion. *Prog. Energy Combust. Sci.* **10**, 1-57.

WILLIAMS, F. A. 1985 Combustion Theory. *Addison-Wesley 2nd Ed.*

WRAY, A. A. 1990 Mimimal Storage Time-Advancement Schemes for Spectral Methods. Private communication.

YU, C. L., FRENKLACH, M., MASTEN, D. A., HANSON, R. K. & BOWMAN, C. T. 1994 Reexamination of Shock-Tube Measurements of the Rate Coefficient of $H + O_2 \rightarrow OH + O$. *Journal of Physical Chemistry.* **98**, 4770-4771.

ZEL'DOVICH, Y. B. 1948 Theory of Flame Propagation. *Zhur. Fizi. Khi. (USSR).* **22**, 27-49.